

TEVATRON RUN-II BEAM COLLIMATION SYSTEM *

M. Church, A. I. Drozhdin, A. Legan, N. V Mokhov[†], R. Reilly, FNAL, Batavia, IL

Abstract

Based on realistic Monte-Carlo simulations a two-stage beam collimation system is designed to minimize the beam loss in the Fermilab Tevatron for fixed target and collider Run II. Thin primary collimators are used to increase particle amplitude and their impact parameter on the downstream secondary collimators. This results in a significant reduction of the total beam loss in the machine, decreases collimator overheating and mitigates requirements to collimator alignment. A set of collimators will originally be installed for fixed target operation and for antiproton beam recycling studies. The collimation system improvement will continue into the collider Run II and intensity upgrade.

1 INTRODUCTION

Even in good operational conditions, a finite fraction of the beam will leave the stable central area of accelerator because of beam-gas interactions, intra-beam scattering, proton-antiproton interactions in the IPs, RF noise, ground motion and resonances excited by the accelerator elements imperfection. These particles produce a beam halo. As a result of halo interactions with limiting aperture, hadronic and electromagnetic showers are induced in accelerator and detector components causing accelerator related background in the detectors. A new collimation system has been designed for the Tevatron Run II to localize most of the losses in the straight sections D17, D49, E0, F17, F48, F49 and A0. In the beginning of Run II a set of collimators will be installed for magnet protection at Fixed Target operation, and for antiproton beam recycling studies. The collimation system improvement will continue for the Collider run and intensity upgrade. A multi-turn particle tracking through the accelerator and beam halo interactions with the collimators are done with the STRUCT[1] code. Using the calculated beam loss distribution, Monte-Carlo hadronic and electromagnetic shower simulation, secondary particle transport in the accelerator and detector components, including shielding with real materials and magnetic fields are done with the MARS[2]code.

2 RUN-II COLLIMATION SYSTEM

The collimation system consists of horizontal and vertical primary collimators and a set of secondary collimators placed at an optimal phase advance, to intercept most of particles out-scattered from the primary collimators during the

first turn after beam halo interaction with primary collimators. An impact parameter on the primary collimators is of the order of $1\mu\text{m}$ [3]. Our studies show that in the Tevatron, a 5-mm thick tungsten primary collimator positioned at 5σ from the beam axis in both vertical and horizontal planes would function optimally, reducing the beam loss rates as much as a factor of 4 to 10 compared to the system without such a scatterer. Secondary collimators located at the appropriate phase advances, are a 1.5 m long L-shaped steel jaw positioned at 6σ from the beam axis in horizontal and vertical planes. They are aligned parallel to the envelope of the circulating beam.

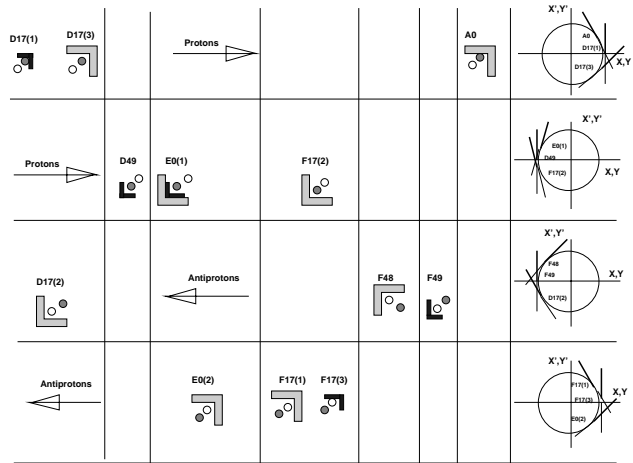


Figure 1: Tevatron Run II beam collimation system.

Based on the Tevatron experience[4, 5, 6], numerous optimization studies, designed helix separation[7] and available space in the Tevatron lattice, the collimation system shown in Fig. 1 is proposed for Run II. A proton primary collimator is placed at the beginning of the D17 straight section outward and up of the closed orbit (Fig. 2). It intercepts the large amplitude protons and a positive off-momentum beam.

Protons scattered from this collimator are presented by a vertical line in the transverse phase diagram (Fig. 1). Protons with a positive angle are intercepted by a D17(3) secondary collimator at the end of the D17 straight section. An A0 secondary proton collimator positioned outward and up of the circulating beam is intended to intercept the negative angle protons emitted from the primary collimator. A primary collimator D49 and secondary collimators E0(1) and F17(2) are used to deal with the protons with negative momentum deviations. Antiproton beam cleaning consists of primary collimators F49, F17(3) and secondary collimators D17(2), F48, F17(1) and E0(2).

* Work supported by the Universities Research Association, Inc., under contract DE-AC02-76CH00300 with the U. S. Department of Energy.

[†] Email: mokhov@fnal.gov

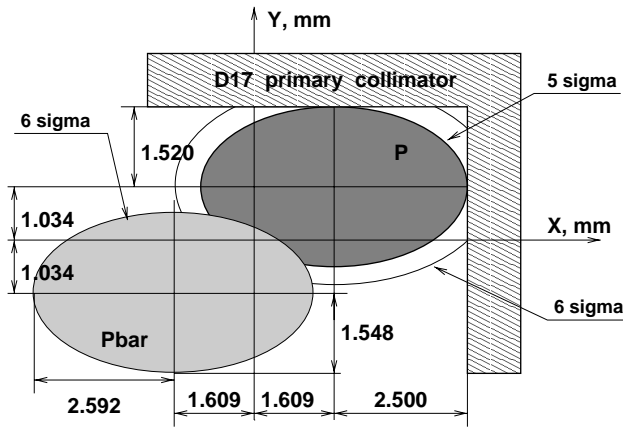


Figure 2: Proton primary collimator D17(1).

3 COLLIMATOR PERFORMANCE

The source of beam halo intercepted by the collimation system is elastic and diffractive $\bar{p}p$ collisions in $B\emptyset$ and $D\emptyset$, intra beam scattering, beam-gas interactions, ground motion, RF noise and resonances. The inelastic and elastic $\bar{p}p$ cross sections at 2 TeV are equal to 60 mb and 15 mb, respectively. The average luminosity is assumed to be equal to $10^{32} \text{cm}^{-2} \text{s}^{-1}$ and antiproton intensity reduction of 60% over the store (10 hours). Table 1 represents our assumptions on the Tevatron intensity evolution.

Table 1: Tevatron intensity evolution over the store

	proton, 10^{11}	antiproton, 10^{11}
Initial intensity	97.2	10.8
Inelastic interactions in $D\emptyset$ and $B\emptyset$	4.32	4.32
Elastic interactions in $D\emptyset$ and $B\emptyset$	1.08	1.08
60% intensity drop		6.48
A drop fraction due to elastic beam-gas interactions, ground motion and resonances		$6.48 - 4.32 - 1.08 = 1.08$ 10% of the beam
10% drop for proton beam	9.72	
Total proton intensity drop	$9.72 + 4.32 + 1.08 = 15.12$	
Intensity at the end of the store	82.08	4.32
Number of particles intercepted by collimators	$1.08 + 9.72 = 10.8$	$1.08 + 1.08 = 2.16$
Scraping rate	3×10^7 p/s	6×10^6 p/s

Halo particles first hit the primary collimator with a 1 to 3 μm impact parameter. On the next turns, the impact parameter—as a result of scattering—increases to about 0.3 mm. The halo horizontal phase space at the D17(3) secondary collimator is shown in Fig. 3 for the off-momentum protons. The ellipse represents a 6σ envelope of the equilibrium energy beam. The vertical line shows the collimator jaw position. After the first interaction with primary collimator high amplitude particles are intercepted by the secondary collimators, but large number of particles survive.

Some fraction of the halo is not intercepted by a primary/secondary collimator pair and will interact with a primary collimator on the next turns. On average, halo pro-

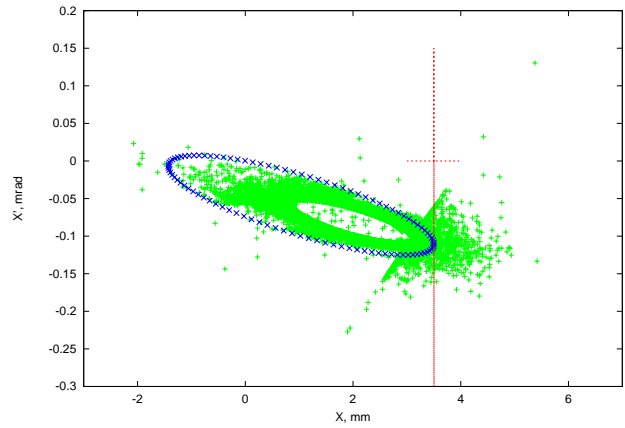


Figure 3: Beam halo horizontal phase space in D17(3) for positive off-momentum collimation.

tons interact with the primary collimator 2.2 times. Particles with the amplitudes $\leq 6\sigma$ are not intercepted by the secondary collimators and do survive for several tens of turns until they increase amplitude in the next interactions with the primary collimator. The tail of halo is extended above 6σ (Fig. 4). Large amplitude particles, which escape from the cleaning system at the first turn, are able to circulate in the machine, before being captured by the collimators on the later turns. This defines the machine geometric aperture. Calculated beam loss distribution in the Tevatron is presented in Fig. 5 for the proton and antiproton directions.

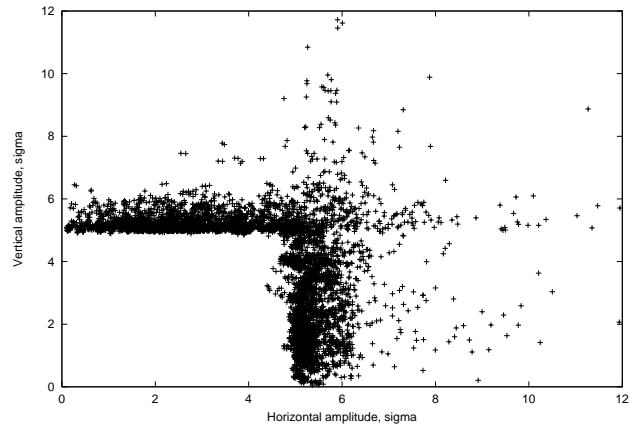


Figure 4: Proton beam halo in the Tevatron aperture.

The studies[6] have shown that the accelerator related background in the $D\emptyset$ and CDF collider detectors is originated by the beam halo loss in the inner triplet region. In addition to the optically small aperture at β_{max} location, the aperture restrictions in this area are the $D\emptyset$ forward detector's Roman pots placed at 8σ and the $B\emptyset$ Roman pots placed at 10σ at the entrance and exit of the beam separators. Beam loss in the $B\emptyset$ and $D\emptyset$ depends strongly on the secondary collimator offset with respect to the primary

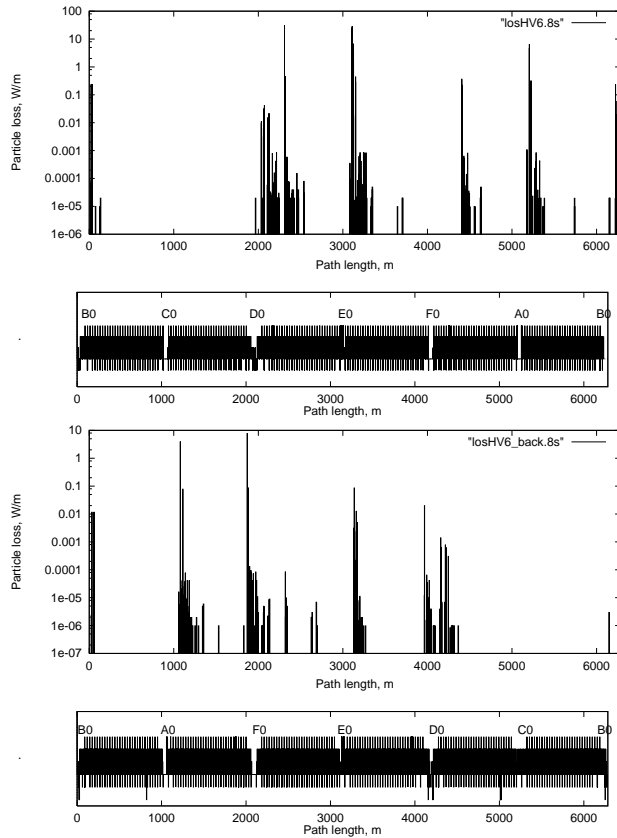


Figure 5: Beam loss in Tevatron at collimation with primary collimators at 5σ and secondary collimators at 6σ for proton (top) and antiproton (bottom) directions.

collimators. Table 2 gives the number of particles passed through the Roman pot detectors for different positioning of the secondary collimators. Beam loss at $D\emptyset$ goes down by a factor of 3 and 6 with the secondary collimators moved from 7σ to 6σ and 5.5σ , respectively.

Before being intercepted by the secondary collimators some of halo particles can pass through the Roman pot detectors several times creating false hits there and additional background in the main CDF and $D\emptyset$ detectors. Background is decreased by a factor of 1.8 if the $D\emptyset$ Roman pots are moved from $8\sigma_x$ to $9\sigma_x$, and by a factor of 1.6 in the CDF detector if the Roman pots at $B\emptyset$ are moved from $9\sigma_x$ to $10\sigma_x$ (Table 2). This would certainly decrease the Roman pot acceptances, therefore their transverse positions have to be chosen as a compromise between the main detector background and forward detector acceptance. The efficiency of collimation in the Tevatron Run II calculated as a ratio of background in the detectors without collimation and with collimation is equal to 150.

4 COLLIMATOR POSITION CONTROLS

The stepping motors (200 steps/turn) will be used to control position of the primary collimators and upstream and downstream ends of the secondary collimators in horizon-

Table 2: Halo hit rate (in $10^5 p/s$) at the $D\emptyset$ and CDF Roman pots for several secondary collimator and pot positions with respect to the closed orbit

Collimators	$5.5\sigma_{x,y}$	$6\sigma_{x,y}$	$7\sigma_{x,y}$	$6\sigma_{x,y}$	$6\sigma_{x,y}$
$D\emptyset$ pots	$8\sigma_{x,y}$			$9\sigma_{x,y}$	$8\sigma_{x,y}$
CDF pots	$10\sigma_{x,y}$			$10\sigma_{x,y}$	$9\sigma_{x,y}$
ROMAS	2.86	5.67	17.9	3.23	5.83
ROMAQ	2.69	5.27	16.5	2.91	5.34
ROMPQ	2.29	4.13	12.3	2.19	4.11
ROMPS	2.31	4.31	12.4	2.39	4.35
CDFPQ	3.11	5.62	9.40	5.75	9.15
CDFPS	4.02	7.49	13.2	7.83	12.5
CDFAS	5.84	10.7	23.5	11.7	17.1
CDFAQ	4.18	8.38	17.2	8.68	13.9

tal and vertical plane independently. The motors will be geared so that the collimator can be moved at a maximum speed of 2.5 cm in 10 seconds, which is approximately the distance from the full out position to the beam axis. This gearing will yield a minimum step size of $3 \mu\text{m}$, which is never larger than about 1/80th of the beam sigma. Position read-back is provided for primary and secondary collimators. Limit switches will protect hardware from damage. Local fast feedback for the motion control will be provided by standard Tevatron loss monitors, placed downstream and upstream of each collimator.

5 ACKNOWLEDGMENTS

We express our gratitude to P. Bagley, D. Finley, J. Marinier, M. Martens, C. Moore, and S. Pruss for useful discussions.

6 REFERENCES

- [1] I. Baishev, A. Drozhdin, and N. Mokhov, "STRUCT Program User's Reference Manual", SSCL-MAN-0034 (1994).
- [2] N. V. Mokhov, "The MARS Code System User Guide, Version 13(95)", Fermilab-FN-628 (1995); N. V. Mokhov et al., Fermilab-Conf-98/379 (1998); LANL Report LA-UR-98-5716 (1998); *nucl-th/9812038 v2 16 Dec 1998*; <http://www-ap.fnl.gov/MARS/>.
- [3] M. Sidel, "Determination of Diffusion Rates in the Proton Beam Halo of HERA", DESY-HERA 93-04 (1993).
- [4] A. I. Drozhdin, M. Harrison, and N. V. Mokhov, "Study of Beam Losses During Fast Extraction of 800 GeV Protons from the Tevatron", Fermilab-FN-418 (1985).
- [5] S. M. Pruss, "A Design for a Beam Halo Scraper System for the Tevatron Collider", Proceedings of the 1991 IEEE Particle Accelerator Conference, p. 2340-2341, May 6-9, San Francisco, California (1991).
- [6] J. M. Butler, D. S. Denisov, H. T. Diehl, A. I. Drozhdin, N. V. Mokhov, D. R. Wood, "Reduction of TEVATRON and Main Ring Induced Backgrounds in the $D\emptyset$ Detector", Fermilab-FN-629 (1995).
- [7] P. Bagley, "Beam Separation for the Tevatron Run-II", Private communication (1998).